A Method for Predicting Nonperiodic Air Loads on a Rotary Wing

LEONARD SEGEL*
Cornell Aeronautical Laboratory Inc., Buffalo, N. Y.

A numerical description of the geometry and strength of the vorticity in the wake of a rotary wing is employed to compute the wake-induced, nonuniform flowfield in the plane of the rotor disk. In contrast to the procedure developed previously to obtain the periodic inflow that exists in steady, forward flight, a solution procedure is adopted appropriate to the treatment of transient phenomena, such as the nonperiodic loadings caused by time-varying control inputs or gust disturbances. Major assumptions made in the analysis are: 1) the rotor blades have only a rigid flapping degree of freedom; 2) the rotor hub continues to translate in level, constant-speed flight during the short time interval of interest; 3) the wake geometry can be specified a priori; and 4) no account need be taken of vorticity shed parallel to the trailing edge of the blades. Computed flapping and air load distributions are compared with wind-tunnel measurements (on a full-scale H-34 rotor) of the response to rapid changes in collective pitch.

Introduction

ACCURATE predictions of the aerodynamic loading on a rotary wing require that the airflow through the rotor be determined in considerable detail. The recognition of this requirement was given significant impetus as a result of measurements made in 1947 at the Cornell Aeronautical Laboratory Inc. (CAL) revealing the presence of fifth and higher harmonic stresses in helicopter rotor blades. No attempt shall be made here to recount the many efforts that were made at CAL and elsewhere[1-9] to obtain methods for predicting the higher harmonic components of air loads which stem from the highly variable inflow experienced by a rotor in forward flight. Since this variable inflow results from the induced-velocity field created by the wake of the rotary wing, a scheme for predicting the aerodynamic loadings on a rotor must necessarily take into account the complex details of the rotor-wake interaction process.

The analysis to be described herein is one of many efforts that have been and are currently being made to derive rational and valid procedures for predicting the results of this complex rotor-wake interaction process.[1-12] The objective of this particular study was the modification and extension of methods previously developed for the case of steady forward flight[13] in order to permit the computation of nonperiodic (or transient) loadings caused by nonperiodic changes in blade-pitch controls or any other type of transient disturbance. Accordingly the analysis may be viewed as a first step towards developing means for computing the transient airloadings encountered by a helicopter rotor as a result of control action applied for maneuver purposes or as a result of entering a gust environment.

Features and Assumptions of the Analysis

Except for the absence of means for computing the induced-velocity field caused by the presence of a vortical wake, Gessow and Crim[14] developed a computing program in 1955 that can be considered a prototype of the program developed in this investigation. In fact, the present effort may be viewed as a logical extension of the analysis performed by these earlier investigators. Specifically, their classical assumption of uniform inflow has been eliminated to the end that the high-frequency components of blade loading (due to the presence of the spiral, vortical wake[15]) can be predicted with accuracies sufficient for engineering purposes.

The air loads on a rotary wing are described mathematically by an integral equation that expresses the requirement for flow tangency to the blade surface as a function of the circulation (vorticity) distributed over the surface of the blade and in the vortex sheet trailed by the individual blades of the rotor. Obviously, the lifting-surface formulation for the rotary wing is considerably more complex than that for the fixed wing because of the complex wake geometry that prevails. Since a helicopter rotor blade has a very high aspect ratio, the classical simplification made by Prandtl is valid, thus permitting the use of lifting line theory in treating this problem. Accordingly, significant success has been achieved in determining the bound circulations that must prevail in steady, level flight in order that the boundary condition of flow tangency be satisfied at one chordwise position on the blade.[3-5, 7-9, 11-13] The key to this success has been a willingness to assume that the geometry of the wake can be specified a priori. Specifically, we assume that the geometry of the wake is determined by 1) the kinematics associated with a given advance ratio and 2) the mean, induced inflow velocity, which velocity is a function of the average rotor lift as defined by simple momentum theory. Application of the Biot-Savart Law to the specified geometry yields a matrix of influence coefficients, by means of which it becomes possible to solve for the spanwise and azimuthal distribution of the bound circulation on the rotor blades. Alternatively, it is possible to solve for the spanwise and azimuthal distribution of angle of attack. Although the flow environment seen by a spanwise segment of the blade is not steady and completely two dimensional, it is consistent with lifting-line theory and the assumption of quasi-steady aerodynamics to employ two-dimensional airfoil-section data to compute the resulting air loadings. The assumption of two dimensionality obviously restricts this model to low advance ratios in which the spanwise component of flow remains small.

In computing transient air loadings, we have elected to model the rotor and wake in essentially the same format that was adopted by Piziali and DuWaldt[13] for steady-state (periodic) loading calculations. As indicated in Fig. 1, each blade of the rotor is represented by a segmented lifting line (bound vortex) located along the quarterchord of the blade with the wake represented by a mesh (or lattice) of straight

Presented as Preprint 66-17 at the AIAA 3rd Aerospace Sciences Meeting, New York, New York, January 24–26, 1966; submitted January 24, 1966; revision received June 6, 1966. Based on work performed for the U. S. Army Aviation Material Laboratories under Contract DA 44-177-AMC-77(T).

* Staff Scientist, Applied Mechanics Department. Member AIAA.

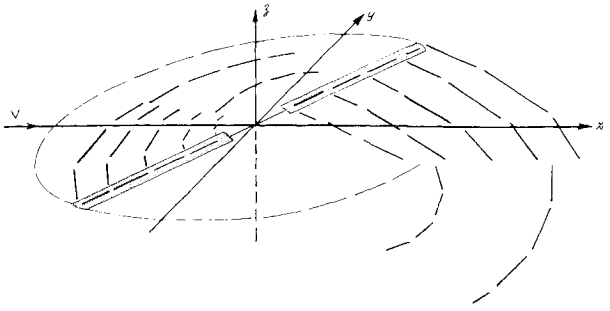

Fig. 1 Example of wake trailed from four radial segments with roll-up into a root and tip vortex.

vortex segments possessing a constant strength over the length of the segment.

In contrast to Ref. 13 the wake model adopted for transient air load calculations is assumed to consist only of trailing vorticity. Obviously, the omission of shed vorticity is equivalent to ignoring the influence of any "unsteady aerodynamic" effects that are associated with the time rates of change of circulation on a two-dimensional segment of the rotor blade. We have elected to make this assumption in view of the results that were obtained in a brief peripheral study (see Ref. 16). This study showed that neglecting shed elements of wake lumped in accordance with the scheme originally adopted,[13] made little difference in loadings calculated for the case of steady, level flight. It was concluded that the procedure used for lumping the shed elements of vorticity did not account for the true influence of the nearby sheet of shed vorticity, and therefore there was no merit in retaining this feature of the original wake model.†

Since it was desirable that 1) the computation time associated with the application of the Biot-Savart Law be minimized and 2) a more realistic simulation be made of the rolling-up process associated with the strong tip and root vortices, the original wake format was appropriately modified (see Fig. 1). Numerical studies showed that the desired gains in calculation efficiency were achieved, and comparisons with experimental results have demonstrated that additional gains accrue from simulation of the rolling-up process. Although insufficient cases were tested to demonstrate the influence of wake contraction on the loadings achieved in forward flight, hovering calculations showed that serious errors are obtained in loading predictions if wake contraction is ignored. Figure 2 shows that when wake contraction is assumed to be nil, a total load and spanwise distribution are calculated which do not agree with results measured on an H-34 helicopter.[17] We also see the significant improvement in the calculated result that is obtained when a rolled-up tip and root vortex are assumed to be located at $r/R = 0.825$ and $r/R = 0.425$, respectively. Although the root vortex appears to have a significant influence on the load distribution in hover, other studies[12] have shown that the root vortex can be ignored when the wake is convected away from the rotor in forward flight.

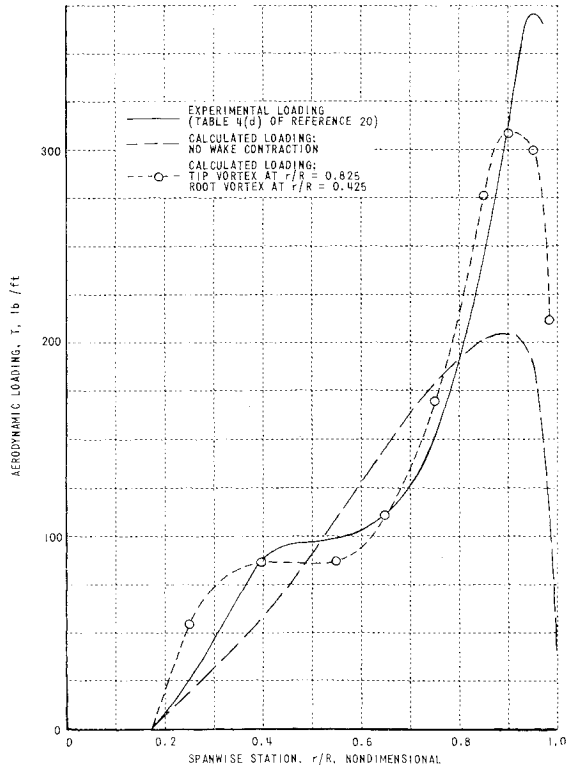

Fig. 2 Comparison of calculated and measured loadings in hovering flight.

As has been mentioned already, a most important feature of the wake model that has been adopted for calculating air loadings on a rotary wing is the requirement to specify the geometry of the wake. In practice, this means that the wake generated in steady, forward flight is considered to be a skewed spiral with the pitch of the spiral determined by a "transport" velocity taken to be the momentum-theory value of the mean induced velocity. (Note that this assumption has been shown to yield calculated azimuthal and spanwise variation of loadings in reasonable agreement with experiment.[13])

In specifying the geometry of the wake generated during a transient maneuver, several problems arise. First, we encounter the question of how to specify a geometry (during the transient interval) that is the equivalent of the "rigid" wake spiral assumed to exist in steady, forward flight. Second, there is the problem of relating the arbitrarily specified wake geometry to the actual dynamics of the flow process wherein the induced air mass is accelerated through the rotor to attain a new mean flow condition.

For purposes of clarifying this point, consider the application of collective blade-pitch control such as to change the average thrust produced by a rotor. It follows that the momentum imparted by the rotor to the mass of air flowing through it must be changed. This is to say that the air mass must be accelerated (or decelerated) until a new steady-state thrust corresponding to the changed operating conditions is achieved. From the point of view adopted in this analysis (namely, that the inflow is induced by the vorticity in the wake), there are time rates of change of inflow that are dependent upon the existence of vortex strengths that are not periodic with respect to the rotor revolution rate. We note that there must be an equivalence between the concept of an air mass being accelerated (during the transient interval between two steady states) and the concept in which a change in vorticity levels is diffused through the wake (during the transient interval) bringing about a change in the velocities induced at the rotor disk.

In the wake model adopted for calculation of transient air loadings, the diffusion of the new vortex strengths‡ is automatically taken into account. For purposes of establishing the geometry that exists between the two rigid skewed spirals that are associated with the initial and the final steady state, we arbitrarily assume that the ends of the vortex elements in the wake are transported downwards at a constant rate. The magnitude of this rate is taken to be the time-varying value of the mean, induced velocity assumed to exist at the specific instant of time that a particular element of vorticity is trailed from the blade. The model, as described, thus re-

† A discussion of the inadequacy of the original procedure used for lumping shed vorticity can be found in Ref. 12. In this study, no attempt was made to employ a scheme for modeling shed wake effects, as developed in Ref. 12.

‡ This is caused, for example, by a change in collective pitch.

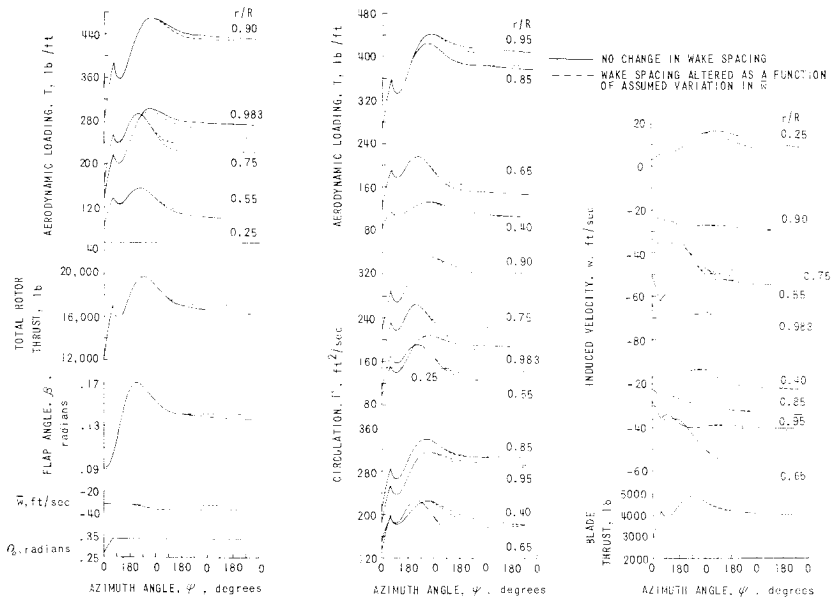

Fig. 3 Transient response to a rapid increase in collective pitch; calculated for the the H-34 rotor in hovering flight.

quired that an assumption be made as to the manner in which the mean, induced velocity, associated with the initial steady state, varies with time to reach the value associated with the final steady state. Accordingly, computations were made for the purpose of assessing the sensitivity of air load responses (as caused by a collective pitch change during hover) to the time history assumed for the mean, induced downwash. These computations showed (Fig. 3) that the form of the loading time histories is not particularly sensitive to the change in wake geometry occurring during the transient interval, although the final steady load magnitudes are, admittedly, a sensitive function of the pitch of the wake spiral as controlled by the assumed final value of the mean, induced velocity.

A number of simplifying assumptions were made in addition to the previously mentioned 1) neglect of shed vorticity and 2) requirement for specifying the time history of the mean, induced flow in relation to the time history of the transient input. These other assumptions are: 3) The bound circulation on a blade segment is proportional to the lift on this segment irrespective of whether the segment is or is not "stalled."§ 4) The lateral and longitudinal components of the velocity induced by the wake are negligibly small in comparison to the tangential velocity and therefore can be ignored in determining the angle of attack of a given blade segment. 5) The rotor blades are structurally rigid and have only a flapping degree of freedom.¶ 6) The rotor revolves at a constant angular velocity throughout the transient interval. 7) The hub of the rotor continues to translate in level, forward flight at constant speed during the short time interval of interest.

With respect to these seven assumptions, it appears that some reservation need be retained as to the adequacy of the first assumption when very rapid changes of bound vorticity are produced as a result of 1) very rapid changes in blade-pitch settings and/or 2) very rapid changes in the induced-velocity field as caused by a blade passing over the tip vortex trailed by a preceding blade. Admittedly, more calculations are in order to assess the quantitative role of shed vorticity during those flight conditions in which unsteady aerodynamic effects would be accentuated.

§ It should be appreciated that the model does accommodate a region of reversed flow but was not intended to yield accurate results for high advance ratios or highly loaded flight conditions.

¶ Work is under way to eliminate this restriction to a rigid blade. It is expected that inclusion of feathering and structural twist will prove to be of importance in calculating rotor air loads.

Computer Program Implementation

Figure 4 diagrams the computational program that was developed to predict the nonperiodic air loadings on a rotary wing. These numerical computations require that an axis system be selected to describe the flapping response of the rotor and the geometry of the wake. Figure 5 shows the x-y-z-axis system adopted for this purpose. Note that the origin is placed at the hub of an articulated (flapping) rotor, with x axis directed rearward, parallel to the horizontal direction of flight. It should be recalled that the analysis is restricted to level-flight operations or to the situation that prevails when the rotor hub is held fixed in a wind tunnel. Figure 6 shows that the rotor shaft has been assumed to be tilted only in the x-z plane. Thus, we ignore any lateral tilt of the rotor shaft, since this tilt angle is usually small during

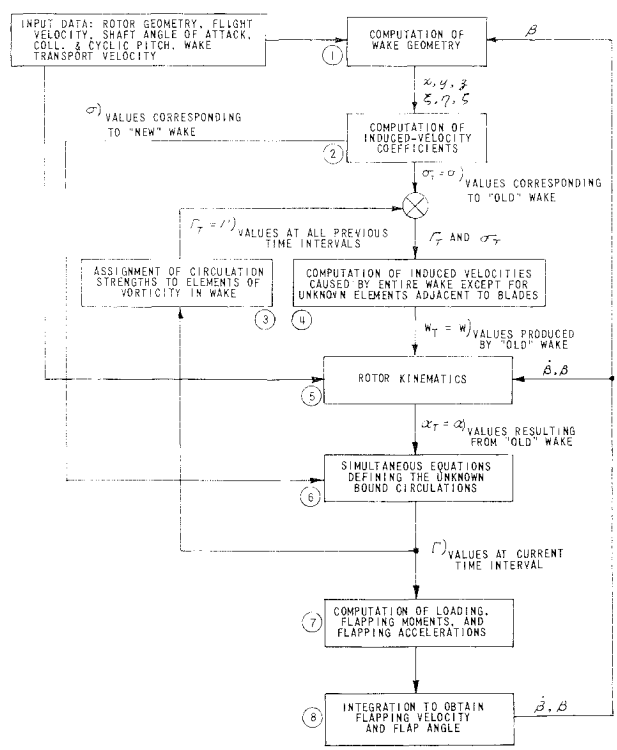

Fig. 4 Schematic diagram of transient blade load model.

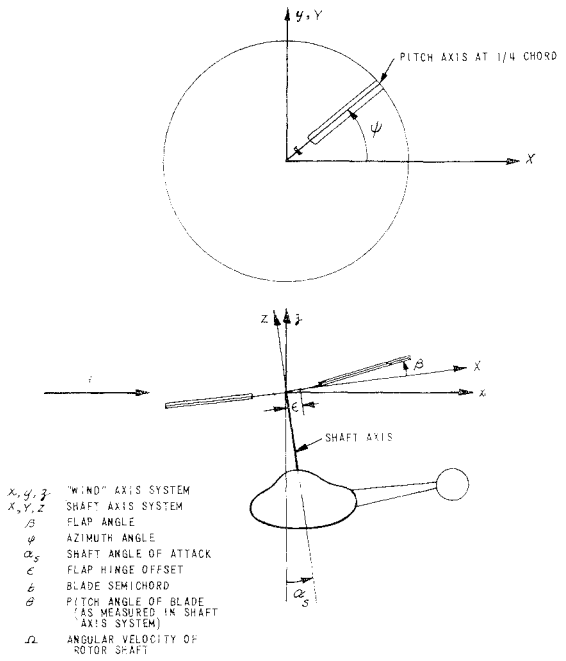

Fig. 5 Axis system used in transient blade load analysis.

trimmed, level flight. A conventional shaft axis system is used to describe the flapping and feathering of the blades, and the motions and displacements of the blades (as seen in the shaft axis system) are transformed to equivalent quantities in the x-y-z system. Only the z axis component of the total induced-velocity vector is included in the analytical model, as was indicated earlier. In accordance with the adopted axis system, velocities induced in the negative z direction are designated as negative quantities.

Using the indexing procedure shown in Fig. 6, m designates an instant of time, i is a blade of the rotor, j is a spanwise location on a blade, ib is the wake trailed by a blade i, $\bar{m}$ is an azimuthal position in the wake, and l is a spanwise position in the wake. Arithmetic statements and indexing logic were written for each of the eight blocks indicated by number in Fig. 4. These eight portions of the program are reviewed and summarized below.

Computation of Wake Geometry

This portion of the program consisted of equations that yield the geometry of the wake, i.e., the spatial location and orientation of elements of vorticity in the wake relative to the blades of the rotor at each instant of time. The azimuthal position in the wake at which the wake is assumed to roll up into two vortices, i.e., one from the blade tip and one from the blade root, is designated as $\bar{m} = MBLM$. With this notation, it becomes convenient to write a separate set of

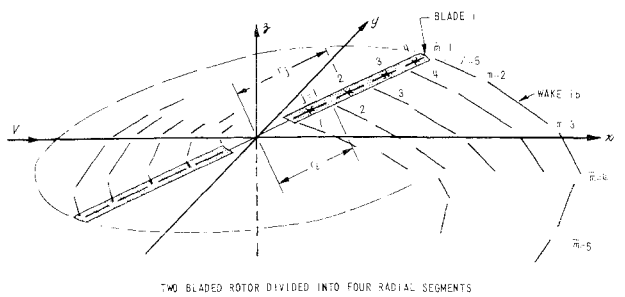

Fig. 6 Indexing procedure used to designate blade and wake geometry.

equations defining the geometry of the nonrolled wake ($\bar{m} \leq MBLM$) and the rolled-up wake ($\bar{m} \geq MBLM$).

Computation of Induced-Velocity Coefficients

The Biot-Savart Law is employed to compute the induced-velocity coefficients representing the velocity induced at a specific location on a blade by a given segment of wake per unit strength of vorticity in the wake element. The induced-velocity coefficient, σ, is a function only of the coordinates of the point where the velocity is being computed and the coordinates of the vortex filament endpoints. A complete set of σ coefficients represents the influence of all of the elements of vorticity in the wake (of unit strength) at all of the spanwise locations selected to define the loading on each blade. It should be noted that Fig. 4 indicates that these velocity coefficients are separated into two parts. One part, σ_T, represents all of the velocity coefficients associated with the entire wake except for the elements of wake immediately adjacent to the trailing edge of the blade. The remainder of the velocity coefficients represent the influence of the adjacent wake and are stored for later use in the computations that are made in block 6.

Assignment of Circulation Strengths to Elements of Vorticity in the Wake

This is primarily a bookkeeping operation in which circulation strengths are assigned to all elements of the wake (except for the elements adjacent to the blades) at each instant of time as a function of the bound vorticities that were determined at earlier instants of time.

Computation of Induced Velocities

For purposes of implementing the transient blade loads computation, the contributions of all vortex elements to the total velocity induced at a blade segment location are summed over the entire wake, with the exception of the elements located immediately adjacent to the blades. The circulation strengths assigned in block 3 and the σ_T portion of the induced-velocity coefficients computed in block 2 are required for this summation. The result of this incomplete summation for the induced velocity is designated as W_T. We have that the velocity induced at time m on blade i at spanwise station j by all elements of the wake, other than the elements adjacent to the blade, is given by

$$W_{T_{m,i,j}} = \sum_{ib=1}^{NB} \left\{ \sum_{m=3}^{MBLM} \sum_{l=1}^{LCN+1} \sigma_{ib,\bar{m},l}^{m,i,j} \left[\Gamma_{ib,m-\bar{m}+2,l} - \Gamma_{ib,m-\bar{m}+2,l-1} \right] + \sum_{\bar{m}=MBLM+1}^{NA(NR)+1} \bar{\Gamma}_{ib,m-\bar{m}+2} \left[\sigma_{ib,\bar{m},1}^{m,i,j} - \sigma_{ib,\bar{m},2}^{m,i,j} \right] \right\} \qquad m \geq 2 \quad (1)$$

where NB = number of blades, LCN = number of blade load points, and NR = number of revolutions of wake retained in the summation. $\sigma_{ib,\bar{m},l}^{m,i,j}$ is the induced-velocity coefficient yielding the influence of the wake element designated by the subscripts ib, $\bar{m}$, and l at the specific location indicated by the superscripts m, i, j. The subscripts on the wake vorticity Γ accomplish the aforementioned bookkeeping process. Note that the right-hand interval summation over $\bar{m}$ is associated with the rolled-up wake, where $\bar{\Gamma}$ refers to the peak value of circulation that existed on a given blade.

Rotor Kinematics

In this portion of the computing program, the blade-segment angles of attack are determined as a function of the kinematics of the rotor and the existing induced-velocity field. It should be noted that the angle of attack as deter-

mined at this point is a function only of the "old wake," that is, that part of the wake that produces the induced velocity W_T.

Simultaneous Equations Defining the Unknown Bound Circulations

The fundamental assumption involved in this portion of the calculation is that the bound circulation on the blade is proportional to the lift coefficient, irrespective of whether the given spanwise segment is or is not stalled. Since the angle of attack at each spanwise station is a function of both the known circulation strengths (which result in the partial induced-velocity field, W_T) and the additional induced velocities caused by the unknown circulation strengths associated with the wake elements that trail immediately behind the blade, we have that the unknown bound circulation on every spanwise segment is a function of all the unknown bound circulations that exist at a given instant of time. Mathematically, this means that a set of algebraic equations must be solved simultaneously to obtain the unknown circulations where the number of unknown circulation strengths to be found at any instant of time is equal to the product of the number of spanwise segments and the number of blades. It should be noted that this set of equations must be solved for as many time intervals as are required to 1) establish an initial equilibrium state, 2) define the transient response to a specified input disturbance, and 3) establish a final equilibrium state.

Since the equation set defining the relationships between the unknown circulation strengths is nonlinear, an iterative scheme was necessarily developed. The solution process is initiated by utilizing a linearized formulation of the problem. The linear equations that result can be indicated symbolically as

$$[\sigma_{ib,l^{m,i}}]_m \{\Gamma_{m,i,j}\} = \{\Gamma_{m,i,j^g}\} \tag{2}$$

where the column matrix $\{\Gamma_{m,i,j}\}$ represents the unknown circulation strengths. The column matrix $\{\Gamma_{m,i,j^g}\}$ represents that portion of the circulation at each spanwise segment as determined by all contributions to the local angle of attack other than the contribution that derives from the so-called "new" wake, which is defined by the unknown circulations. The square matrix $[\sigma_{ib,l^{m,i}}]$ is derived from the velocity coefficients that were computed earlier in block 2 and then stored use for in block 6.

On obtaining a solution to the linearized equation set, the iterative process is initiated by computing the additional induced velocities W_A that are caused by the strengths in the "new" or adjacent wake, viz.,

$$W_{A_{m,i,j}} = \sum_{ib=1}^{NB} \sum_{l=1}^{LCN} \Gamma_{m,ib,l}[\sigma_{ib,2,l^{m,i,j}} - \sigma_{ib,2,l+1^{m,i,j}}] \tag{3}$$

The induced-velocity coefficients in the foregoing expression are the stored quantities from block 2. To iterate, we 1) recompute $\alpha_{m,i,j}$, 2) obtain a new set of lift coefficients, 3) recalculate the bound circulations, 4) recalculate W_A, and 5) continue this loop until the changes computed in $\Gamma_{m,i,j}$ are less than a specified percentage.

Considerable care must be exercised to insure that convergence is obtained since an increase in $W_{A_{m,i,j}}$ (negative for downwash) causes a decrease in $\Gamma_{m,i,j}$ which, in turn, causes a decrease in $W_{A_{m,i,j}}$. Investigation showed that a Gauss-Seidel solution procedure, along with an averaging technique for Γ and W_A, provides rapid convergence to a stable solution.

Computation of Loading, Flapping Moments, and Flapping Accelerations

The lift and drag determined for each spanwise segment are converted to aerodynamic loading, as measured by pressure transducers mounted on the blade. The aerodynamic moment about the flapping hinge is obtained for each blade from a spanwise integration of the appropriate force components and, likewise, the drag moment about the shaft axis is obtained for each blade and for the total rotor. The angular flapping acceleration of each blade follows from a solution of the blade flapping equation, viz.,

$$\ddot{\beta}_{m,i} = \frac{M_{A_{m,i}}}{I_b} - \frac{M_W}{I_b} - \Omega\left(1 + \frac{\epsilon}{g}\frac{M_W}{I_b}\right)\beta_{m,i} \tag{4}$$

Timewise Integration to Obtain Flapping Velocity and Flap Angle

A conventional Runge-Kutta integration procedure was used to integrate $\ddot{\beta}_{m,i}$ to obtain $\beta_{m+1,i}$ and $\beta_{m+1,i}$. It should be noted that this integration involved predictions over the half and full time (azimuth) interval, with W_T being assumed to remain constant over this interval. No attempt was made to include the wake geometry and induced-velocity computations into the Runge-Kutta integration process, since this procedure would have been prohibitive in terms of computing time and cost. Since the coupling between W_T and blade flapping displacement during a single time (azimuth) interval is very small, the errors introduced by removing the W_T calculation from the Runge-Kutta procedure are believed to be negligible.

Results

Comparison of Theory and Experiment

The foregoing computer program was given its particular form to enable the prediction of loading time histories resulting from transient disturbances. However, one measure of the adequacy and validity of this mathematical model is its ability to predict the steady-state loadings that occur in steady, forward flight. Since means for making predictions of the steady, periodic loadings on rotary wings have been discussed fully elsewhere,[1-13] a comparison between theory and measured steady-state loadings is given here only for reasons of demonstrating that the particular simplifying assumptions made to reduce the complexity of the step-by-step integration approach do not degrade the validity and accuracy of the final result.

Figure 7 is a comparison of calculated periodic air loadings, i.e., in steady, forward flight, with data obtained in full-scale wind-tunnel tests.[18] The loadings plotted in this figure correspond to the initial steady-state achieved in the first run of three transient data runs prior to the initiation of a collective-pitch change (See Table 1 for definition of test conditions.) In the calculations, the tip and root vortices were assumed to roll up 45° of azimuth behind the blade at radial locations corresponding to $r/R = 0.90$ and 0.375, respectively. It appears that the agreement achieved between theory and experiment is comparable to that achieved by other investigators and that the noted discrepancies are, in general, of the same nature and order as have been observed on other occasions.

Three transient responses to collective-pitch inputs were obtained at two "flight" conditions, as tabulated in Table 1.** One transient-response run was made at the first flight condition, in which run the collective pitch was increased at a rather slow rate. In the second flight condition, two transients were produced, one in response to a more rapid increase in collective pitch, a second in response to a rapid decrease.

In order to facilitate a comparison between theory and experiment, it was necessary first to reduce the test data for purposes of determining the cyclic-pitch settings and time

** Originally a more exhaustive test program was planned, but instrumentation difficulties forced the curtailment of the transient response tests.

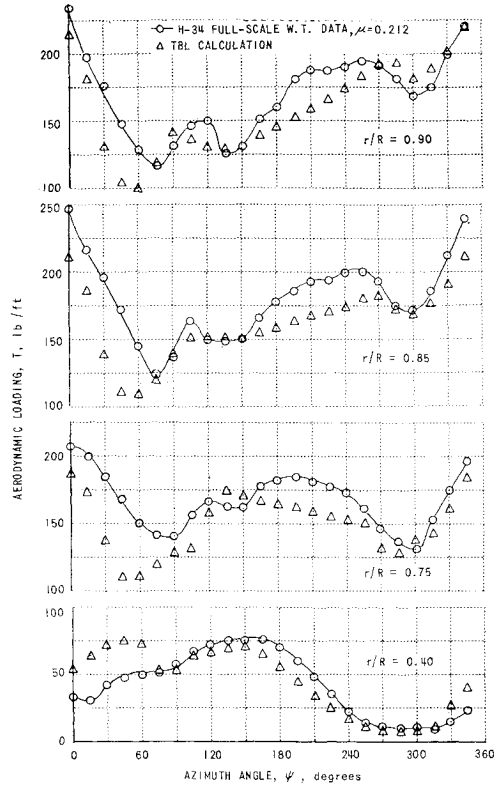

Fig. 7 Steady-state aerodynamic loadings vs azimuth angle.

history of collective pitch. Since blade ptich was measured on blades separated by 180° of azimuth, collective pitch could be resolved by summing the output of these pitch transducers. Cyclic pitch was then determined by subtracting collective from the pitch of the instrumented blade.

Figures 8, 9, and 10 present comparisons of measured and predicted transient air loadings for 7 span positions for test runs 1, 2, and 3, respectively.†† Shown also are predicted and measured flapping, the time history of collective pitch (as measured and as used for the input to the calculation), and the assumed variation in the mean induced velocity $\overline{W}$ governing the spacing of the wake during the steady and transient interval. The assumed timewise variation in $\overline{W}$

Table 1 Wind-tunnel test conditions

	Run 1	Run 2	Run 3
Average test velocity, fps	131.0	186.0	186.5
Rotor angular velocity, rad/sec	23.2	23.2	23.2
Advance ratio	0.202	0.286	0.287
Shaft angle of attack, deg	10	5	5
Average air density, slugs/ft³	0.002293	0.002276	0.002272
Initial total lift, lb	8710	8945	8715
Final total lift, lb	12182	[a]	2037
Total collective-pitch increment, deg	1.775	1.607	−2.663
Rate of change of collective pitch (nominal value) deg/sec	6.55	12.95	−47.2

[a] No wind-tunnel balance reading because of excessive vibration.

†† It should be noted that at $r/R = 0.95$, the calculated response corresponds to $r/R = 0.96$ as a result of using eight segments to define the spanwise load distribution.

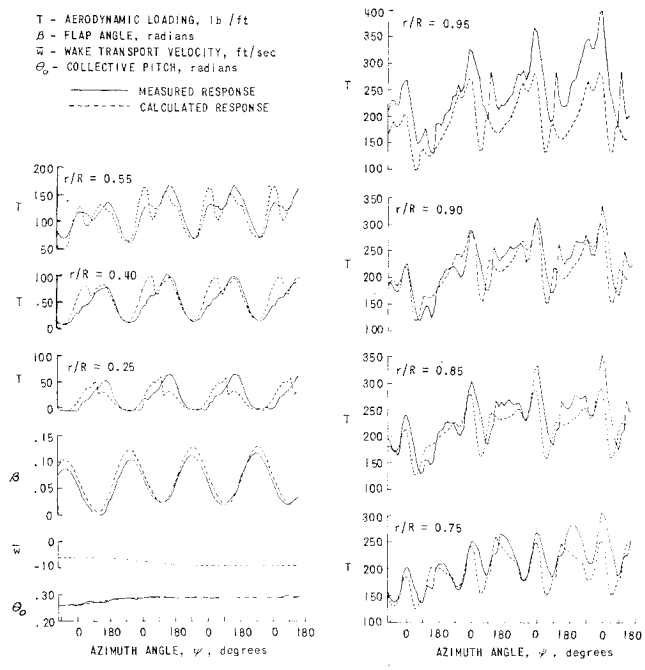

Fig. 8 Measured and calculated transient flapping and air load responses; H-34 rotor, wind-tunnel Run 1, $\mu = 0.202$.

was based on the results of the hovering calculations mentioned earlier. As a result of this hovering study, there is reason to believe that the computed air loadings would not be modified significantly on assuming a different time variation in $\overline{W}$. Instead, it appears that wake distortion arising from self-induced effects, in all likelihood, contributes errors in the description of wake geometry which are considerably more significant than the errors that result from the very approximate means used to simulate the time-varying spacing of the wake spiral during the transient interval.

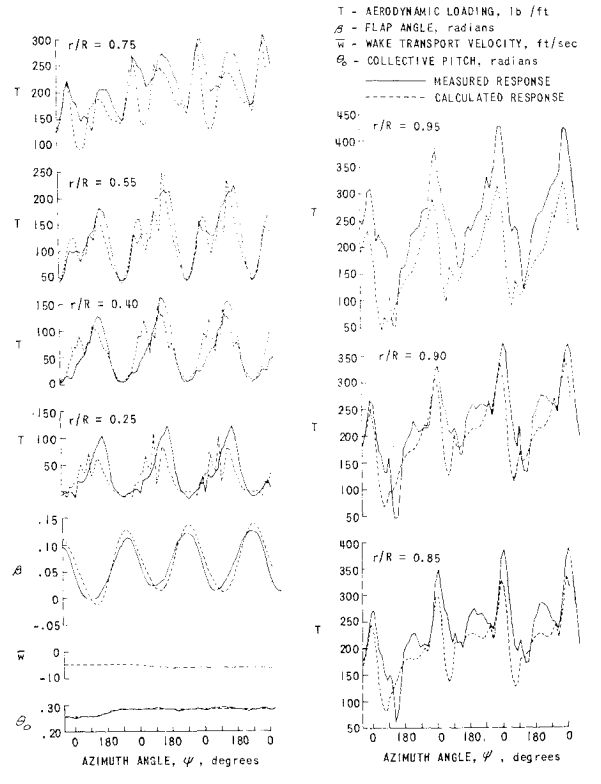

Fig. 9 Measured and calculated transient flapping and air load responses; H-34 rotor, wind-tunnel Run 2, $\mu = 0.286$.

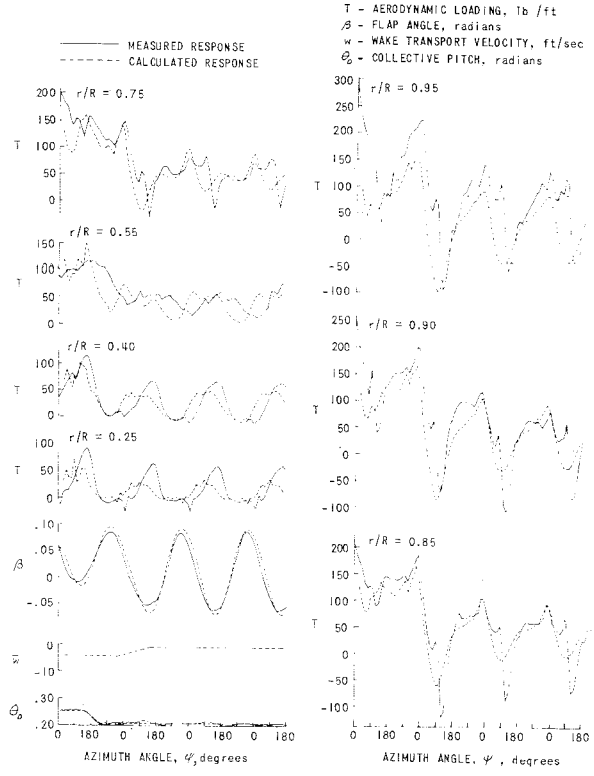

Fig. 10 Measured and calculated transient flapping and air load responses; H-34 rotor, wind-tunnel Run 3, μ = 0.287.

Figures 8, 9, and 10 show that the developed computer model simulates in remarkably good fashion the over-all behavior of a rotary wing subjected to a change in collective pitch. Although the computations do not produce precise agreement with the measured time histories of air loadings, there are many areas of qualitative and quantitative agreement. It is seen that certain portions of the high-frequency content in the loadings are predicted by theory remarkably well. Note should be taken of the agreement between theory and experiment as reflected by the different patterns of loading that occur at the various radial positions on the blade. Note also the agreement achieved between measured and predicted flapping. It is seen that Figs. 8, 9, and 10 do not readily indicate whether discrepancies, if any, exist between the calculated and measured mean loadings. The calculations, as performed, yielded mean total thrusts approximately 4% less than the initial and final mean steady-state thrusts measured for all three runs with one exception; that is, the calculated average thrust for the final steady-state achieved in Run 3 is approximately 2600 pounds (approximately 30% greater than the measured value). These discrepancies in the mean thrust levels obviously do not detract from the basic validity of Figs. 8, 9, and 10 for demonstrating the ability of the transient blade load model to predict variations in air loading, either with respect to spanwise position on the blade or azimuthal location in the rotor disk. It would appear that continued updating of this analysis with respect to 1) refinements in the aerodynamic treatment, 2) improvements in the description of wake geometry, and 3) expanded modeling of the rotor structure will lead to an even better prediction capability. Accordingly, we conclude that the wake model in its present form, together with a model of the kinematics and dynamics of a simple articulated, rigid-blade rotor simulates the essential components of the transient blade loading phenomenon resulting from typical changes in collective pitch. Admittedly, additional data are needed at lower and higher advance ratios in order to confirm and further qualify this conclusion.

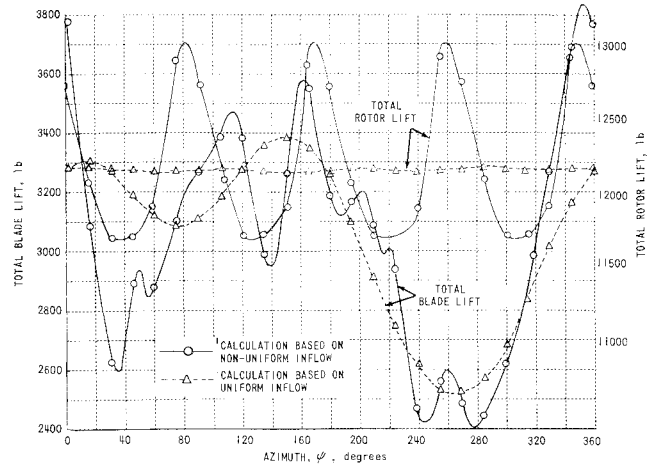

Fig. 11 Total lift on blade and rotor vs azimuth; H-34 rotor, μ = 0.18.

Uniform vs Nonuniform Inflow Calculations

Advantage can be taken of an initialization phase of the calculation, which assumes a fixed inflow, to compare results yielded by uniform- and nonuniform-inflow theory. In Fig. 11, we see the azimuthal variation of total thrust on a single blade yielded by a uniform- and nonuniform-inflow calculation. Also shown are the azimuthal variations in the total thrust of the rotor (as yielded by both calculations) for the same flight condition. Figure 11 graphically exhibits the high harmonic variation in the total thrust of a single blade that derives from the blade-wake interaction process. We also note that the nonuniform-inflow calculation predicts an oscillatory total shear at the rotor hub equal to approximately 10% of the mean thrust, whereas very little oscillatory component is predicted by a uniform-inflow calculation. Obviously, nonuniform-inflow theory has particular significance with respect to calculation of transmitted shears.

Conclusions

This investigation has shown that the existence of high-speed computing equipment makes the prediction of nonperiodic air loadings on rotary wings a feasible task. Although the computation of transient flapping, assuming uniform inflow, required several hours in 1955, the equivalent calculation today requires 3 to 4 min. On the other hand, a numerical simulation of the wake, to provide means of eliminating the uniform-inflow assumption, results in a total computing time (i.e., to reach an equilibrium state) of approximately 15 to 30 min, depending upon the number of rotor blades and the number of wake revolutions retained in the calculations.

Even though certain discrepancies between the theory and experiment still remain to be resolved, it is concluded that a wake model consisting only of trailing-vortex elements, trailed as a consequence of a spanwise variation in bound vorticity, constitutes a first-order representation of the wake of a rotary wing. The achievements reported herein are believed to hold forth the promise of ultimately being able to predict the manner in which 1) performance, 2) maneuver response, 3) vibratory loading and stresses, and 4) response to gust disturbances are modified and controlled by the spiral wake that is peculiar to the rotary wing.

References

[1] Willmer, M. A. P., "The loading of helicopter blades in forward flight," Aeronautical Research Council R & M 3318 (April 1959).

[2] Tararine, S. and Delest, M., "Experimental and theoretical study of local induced velocity over a rotor disc for analytical

evaluation of the primary loads acting on helicopter rotor blades," Giravios Dorand Rept. DE 2012(1960).

[3] Shi-Tsun, V., "The aerodynamic characteristics of a loaded helicopter rotor from a three-dimensional vortex system," Aviotsionnaya Tekhnika Number 1, transl. by M. A. P. Willmer, Royal Aircraft Establishment Library Translation 1013 (1961).

[4] Piziali, R. A. and DuWaldt, F. A., "Computation of rotary wing harmonic air loads and comparison with experimental results," *Proceedings of the American Helicopter Society Eighteenth Annual National Forum* (The American Helicopter Society, New York, 1962).

[5] Miller, R. H., "On the computation of air loads acting on rotor blades in forward flight," J. Am. Helicopter Soc. **7**, 235–254 (1962).

[6] Molyneux, W. G., "An approximate theoretical approach for the determination of oscillatory aerodynamic coefficients for a helicopter rotor in forward flight," Aeronaut. Quart., XIII, (August 1962).

[7] Piziali, R. A. and DuWaldt, F. A., "Computed induced velocity, induced drag, and angle of attack distribution for a two-bladed rotor," *Proceedings of the American Helicopter Society Nineteenth Annual National Forum* (The American Helicopter Society, New York, 1963).

[8] Miller, R. H., "Rotor blade harmonic air loading," AIAA J. **2**, 1254–1269 (1964).

[9] Miller, R. H., "Unsteady air loads on helicopter rotor blades," J. Roy. Aeronaut. Soc. **68**, 217–229 (1964).

[10] Davenport, F. J., "A method for computation of the induced velocity field of a rotor in forward flight, suitable for application to tandem rotor configurations," J. Am. Helicopter Soc. **9**, (1964).

[11] Harrison, J. M. and Ollerhead, J. B., "The nature of limitations imposed on the performance of a helicopter rotor," *Symposium on the Noise and Loading Actions on Helicopter V/STOL Aircraft and Ground Effect Machines*; also J. Sound Vibration (to be published).

[12] Piziali, R. A., "Method for solution of the aeroelastic response problems for rotating wings," Symposium on the Noise and Loading Actions on Helicopter V/STOL Aircraft and Ground Effect Machines; also J. Sound Vibration (to be published.)

[13] Piziali, R. A. and DuWaldt, F. A., "A method for computing rotary wing air load distribution in forward flight," Transportation Research Command Rept. TR-62-44 (November 1962).

[14] Gessow, A. and Crim, A. D., "A method for studying the transient blade-flapping behavior of lifting rotors at extreme operating conditions," National Advisory Committee for Aeronautics TN 3366 (January 1955).

[15] Scheiman, J. and Ludi, L. H., "Effect of helicopter rotor-blade tip vortex on blade air loads," NASA TN D-1637 (May 1963).

[16] Segel, L., "Air loadings on a rotor blade as caused by transient inputs of collective pitch," U. S. Army Aviation Labs., TR 65-65 (October 1965).

[17] Scheiman, J., "A tabulation of helicopter rotor-blade differential pressures, stresses, and motions as measured in flight," NASA TM X-952 (March 1964).

[18] Rabbott, J. P., Jr., "CH-34 Rotor Data," Sikorsky Aircraft Corp., personal communication (March 15, 1965).

[19] *Proceedings of CAL/TRECOM Symposium on Dynamic Problems Associated with Helicopters and V/STOL Aircraft* (Cornell Aeronautical Labs., Buffalo, N. Y., 1963).

NOV.-DEC. 1966 J. AIRCRAFT VOL. 3, NO. 6

Hypersonic Inlet Boundary-Layer Research

JOHN F. STROUD* AND LEONARD D. MILLER†
Lockheed-California Company, Burbank, Calif.

Recent results of a combined analytical and experimental hypersonic inlet boundary-layer research program are reviewed. New turbulent boundary-layer data with heat transfer are presented for a representative compression surface in the Mach number range of 5–8. Surface cooling is shown to have favorable effects on boundary-layer characteristics. The experimental data, with and without cooling, are correlated with a theory developed in this program. The theory has been applied to typical inlets to determine effects of heat transfer and centrifugal forces on basic boundary-layer characteristics as well as on over-all inlet pressure recovery. Both phenomena are favorable, resulting in improved inlet pressure recovery. Centrifugal force effects are more pronounced in low fineness ratio inlets whereas heat transfer effects tend to predominate in high fineness ratio inlets, wherein the supersonic compressive turning is more gradual.

Nomenclature

C_f = local skin friction
h = static enthalpy
H = shape parameter
H_e = shape parameter, δ_e^*/θ_e
H_w = shape parameter, δ_w^*/θ_w
H^1 = total enthalpy
H^* = total enthalpy parameter, $H^1 - h_w$
M = Mach number
P = pressure
q = dynamic pressure
T = temperature
R_e = Reynolds number
u = velocity component along x
u_1 = inviscid velocity component along x
v = velocity component along y
x = distance along surface of body
y = distance normal to body surface
γ = ratio of specific heats
δ = boundary-layer thickness
δ_e^* = displacement thickness, $\int_0 \left(1 - \frac{\rho u}{\rho_e u_e}\right)$ dynes
δ_w^* = displacement thickness, $\int_0^\delta \left(\frac{\rho_1 u_1}{\rho_{1_w} u_{1_w}} - \frac{\rho u}{\rho_{1_w} u_{1_w}}\right)$ dynes
θ_e = momentum thickness, $\int_0^\delta \frac{\rho u}{\rho_e u_e}\left(1 - \frac{u}{u_e}\right)$ dynes
θ_w = momentum thickness, $\int_0^\delta \frac{\rho u}{\rho_{1_w} u_{1_w}}\left(\frac{u_1}{u_{1_w}} - \frac{u}{u_{1_w}}\right)$ dynes

Presented as Preprint 65-605 at the AIAA Propulsion Joint Specialist Conference, Colorado Springs, Colo., June 14–18, 1965; submitted December 6, 1965; revision received June 13, 1966. This research was sponsored in part by the Air Force Flight Dynamics Laboratory, Research and Technology Division, under Contract AF 33(657)-8833 and Lockheed-California Company. R. L. Balent is the RTD Project Engineer.

* Propulsion Department Manager. Member AIAA.
† Research Specialist. Member AIAA.